ORGANOMETALLICS

Article

pubs.acs.org/Organometallics

Functionalization of Sn/S Clusters with Hetero- and Polyaromatics

Eliza Leusmann, Felix Schneck, and Stefanie Dehnen*

Philipps-Universität Marburg, Fachbereich Chemie and Wissenschaftliches Zentrum für Materialwissenschaften, Hans-Meerwein-Straße 4, D-35043 Marburg, Germany

Supporting Information

ABSTRACT: We report a mild and all-purpose method to synthesize several hydrazone-functionalized homo- and heteroaromatic molecules, as well as the attachment of the latter to organic functionalized Sn/S clusters. It turned out that the size of the aromatic system has a great influence on the crystallization tendency of the products, which were characterized by NMR spectroscopy, mass spectrometry, and/or single-crystal X-ray diffraction. The last technique indicates the presence of intramolecular or intermolecular π stacking of the aromatic rings.

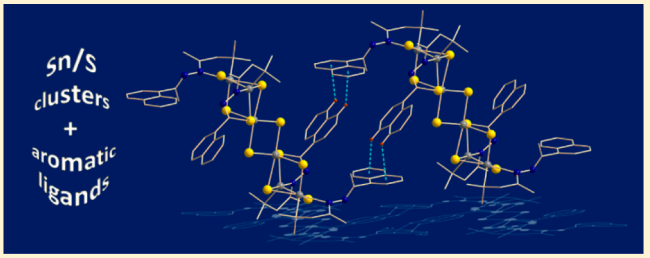

INTRODUCTION

The functionalization of inorganic clusters has been one of the most intriguing goals of cluster chemistry. Three different routes might be discriminated here, at least. The first is where the organic ligand shell has a purely protective role to inhibit thermodynamically preferred particle growth by kinetic stabilization of the (intermediate) cluster.[1] The second is where the organic ligands possess donor atoms or aromatic groups for further coordinative or dispersive interaction with metal atoms, ions, or metal surfaces.[2,3] The third is where the organic molecules possess a functional group, making them reactive toward other molecules with complementary functionality.

One of our current aims is the synthesis and further derivatization of tetrel chalcogenide clusters with organic ligands of the latter class.[4,5] For this, we have been using R^1 = $-CMe_2CH_2C(O)Me$, a keto-functionalized ligand that was introduced for the first time in 1978 as its tin trichloride derivative $Cl_3SnCMe_2CH_2C(O)Me$.[6] On the basis of this, reactions with hydrazine hydrate or organic hydrazine derivatives have allowed for an extension of the ligand shell for different purposes.

A very challenging goal in this context has been the attachment of molecules with chelating groups for (transition) metal ion capture. Generally, the capture of (transition) metal ions can enhance the electronic properties of molecules, such as phosphorescence through Eu(III) and Tb(III) ions in bipyridine ligands on gold nanoparticles, or photon capture in dye-sensitized solar cells through connecting terpyridine units on a silicon surface, adding Fe(II) ions, and saturating them with a further ligand.[7] The first example in this direction was realized by the generation of a bispyridine-functionalized Sn/S cluster capable of sequestering Zn^{2+} ions, which led to the formation of a new Zn/Sn/S/Cl cluster.[8] Another strategy for the installation of metal complexes on a metal chalcogenide cluster surface has been the attachment of preformed (transition) metal complexes, such as ferrocene and ruthenocene, on the surface of inorganic clusters,[9−11] in particular tin oxo clusters,[12] or fullerenes.[13]

Herein, we present a third approach, which deals with the decoration of the cluster with aromatic molecules that can serve as complexing agents. A few molecules have been known to bear Sn atoms and aromatics.[14] In an extension of preliminary work with phenyl or bis-naphthyl groups as simple homoaromatic ligands,[4,15] we first concentrated on further (poly)-homoaromatic groups such as benzyl, mononaphthyl, and anthracenyl groups and continued the study by introduction of heteroaromatic moieties such as quinolinyl groups.

RESULTS AND DISCUSSION

Upon synthesis of hydrazones from aromatic aldehydes or ketones by a newly developed, mild, and universally applicable method, all of these hydrazones (and a commercially available hydrazine derivative) were reacted with the Sn/S cluster **A** with stirring at room temperature to form Sn/S clusters with new aromatic ligands. The title compounds comprise the first examples of Sn/S clusters that are decorated by heteroaromatic or polyaromatic molecules. For the latter, we have observed a clear decrease in the tendency to form single crystals with an increasing number of aromatic rings (e.g., phenyl > naphthyl > anthracenyl/phenanthryl derivatives). It is so far unclear whether a suitable packing of the molecules is hampered by ever bulkier ligands that may not be in a position to realize the desired π-stacking interaction or whether stronger interactions in solution inhibit crystallization.

A rearrangement of the inorganic cluster core occurs along with all reactions, as a consequence of the size and rigidity of the molecules used for the organic ligand extension, as previously observed for the attachment of further bulky

Received: April 8, 2015

DOI: 10.1021/acs.organomet.5b00295
Organometallics XXXX, XXX, XXX−XXX

Scheme 1. Condensation Reaction at the Organic Groups of A, Given for Hydrazones as Reactants[a]

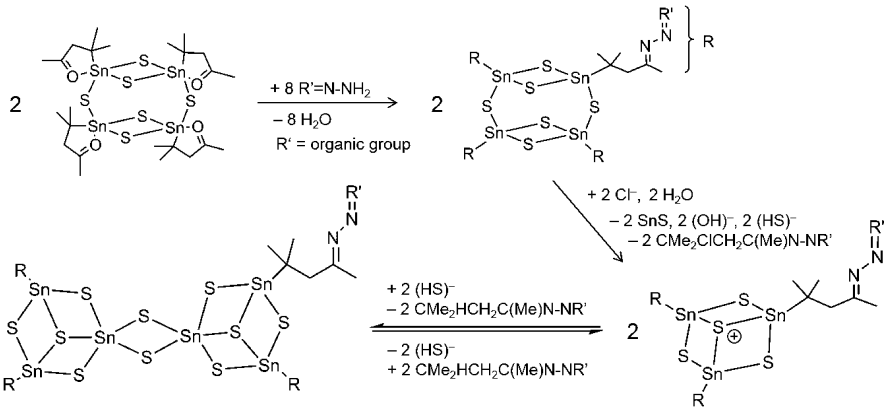

[a]The step is instantly followed in situ by rearrangement into a corresponding defect-heterocubane cation, which reversibly aggregates to a doubly μ-S bridged "dimer" of defect-heterocubane units. Cl^- ions stem from the solvent CH_2Cl_2. All given side products were identified by standard analytical methods.

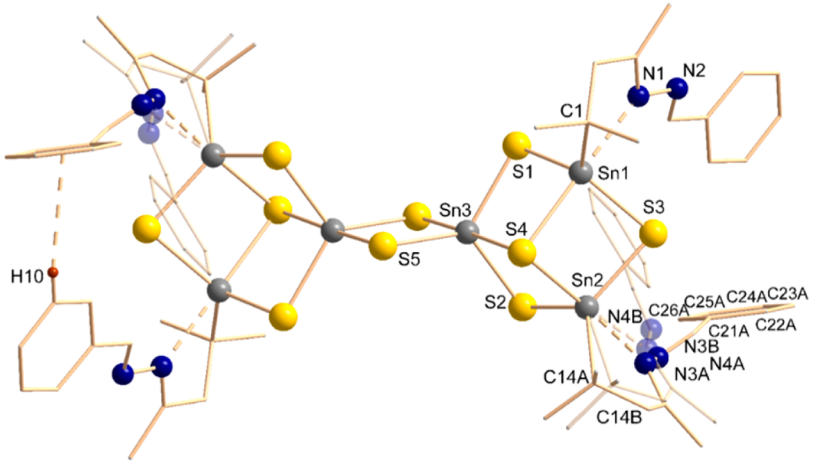

Figure 1. Molecular structure of the cluster in **6** with disorder in transparent mode. Thermal ellipsoids are shown with 50% probability, organic moieties are shown as wires, and H atoms are omitted for clarity. Atom color code: yellow, S; gray, Sn; blue, N; red, H. H10 shows an interaction with one of the disordered aromatic rings (C21A–C26A).

ligands.[4,5,8,9] Hence, instead of the composition and topology of **A**, all clusters reported herein are based on defect-heterocubane-type $[Sn_3S_4]$ moieties, as confirmed by the detection of $[(RSn)_3S_4]^+$ species by ESI^+ mass spectrometry (see the Experimental Section) and/or crystal structures. Single crystals suitable for X-ray diffraction (see Table S1 in the Supporting Information) were obtained for compounds **6**–**8** and **10**, which indicate crystallization of the compounds as two doubly μ-S bridged defect-heterocubane units $[(RSn)_4Sn_2S_{10}]$, thus a "dimeric" arrangement, which cannot be retained under ESI-MS conditions in agreement with our previous findings.[4,5,8,9] An equilibrium is likely to exist in solution with differing amounts of the respective "monomeric" or "dimeric" species, as a function of the nature and bulkiness of the terminal ligands and the corresponding stability and solubility of the resulting clusters (Scheme 1). According to our observations to date, including NMR data, the larger, neutral cluster has the overall higher crystallization tendency, while the smaller, cationic cluster is usually predominant in solution.

In the crystal structures, two of the Sn atoms per inorganic subunit bind to the organic ligands, whereas the third Sn atom is exclusively coordinated by S^{2-} ligands and is part of the $[Sn_2S_2]$ junction of the two subunits. Each Sn atom is surrounded in a distorted-trigonal-bipyramidal manner, either by one C atom, three S atoms, and one intramolecular N coordination or by five S atoms, respectively. The distortion of the trigonal bipyramids is more severe around the latter, "inorganic" Sn atom.

The benzyl-decorated Sn/S cluster in **6** (Figure 1) crystallizes in the triclinic space group $P\bar{1}$ with one formula unit per unit cell. The Sn–S distances (Table S2 in the Supporting Information) in the molecular structure of the centrosymmetric cluster vary between 2.3830(19) Å (Sn3–S5) and 2.819(2) Å (Sn3–S4), with the shortest and the longest bonds being cis to each other.

Sn–C distances (2.174(7)–2.32(29) Å) and Sn–N distances (2.420(6)–2.50(2) Å) are in the expected range. Due to the formation of five-membered rings with the organic ligands, which do not allow for 90° angles between the two Sn-bonded atoms (75.4(3)–76.9(7)°), the trigonal bipyramids around the organyl-substituted Sn atoms Sn1 and Sn2 are slightly distorted. Equatorial angles are 100.0(6)–124.0(5)° (C–Sn–S) and 91.02(7)–115.91(8)° (S–Sn–S); the apical atoms (N, S) are oriented at angles of 169.6(6)–179.22(16)°. The distortion of the coordination sphere around the "inorganic" Sn3 atoms is reflected in equatorial or axial S–Sn–S angles of 85.03(6)–

DOI: 10.1021/acs.organomet.5b00295
Organometallics XXXX, XXX, XXX–XXX

123.29(7) and 178.30(6)°, respectively. The orientation of the phenyl rings within each of the $[Sn_3S_4]$ units allows for an intramolecular T-shaped C−H···π interaction involving H10.

The packing of the molecules within the crystal (Figure S7 in the Supporting Information) produces alternating layers that comprise the inorganic parts of the clusters which are separated by the aromatic rings, indicating further interactions between the latter.

The 1-(naphthalen-1-yl)ethylidene)-decorated cluster in **7** (Figure 2) crystallizes with four formula units and six molecules of CH_2Cl_2 per formula unit in the monoclinic space group $C2/c$. The Sn−S distances (Table S2 in the Supporting Information) vary between 2.390(2) Å (Sn3−S5) and 2.711(2) Å (Sn3−S4); thus, in agreement with **6**, the shortest and the longest bonds are in positions cis to each other. Again, Sn−C (2.179(7)−2.184(8) Å) and Sn−N distances vary only slightly (2.367(7)−2.399(7) Å). A distortion of the trigonal-bipyramidal coordination around the Sn atoms with Sn−C bonds comes along with the "bite" of the atoms within the five-membered Sn−C−C−C−N− ring (N−Sn−C 75.4(3), 75.9(3)°); equatorial atoms include angles of 100.1(2)−128.9(2)° (C−Sn−S) and 90.85(8)−114.81(8)° (S−Sn−S), and the "linear" groups show N−Sn−S angles in the range 174.38(16)−179.11(18)°. The SnS_5 moieties exhibit S−Sn−S angles of 85.90(7)−128.96(8)° (equatorial) or 175.46(7)° (axial).

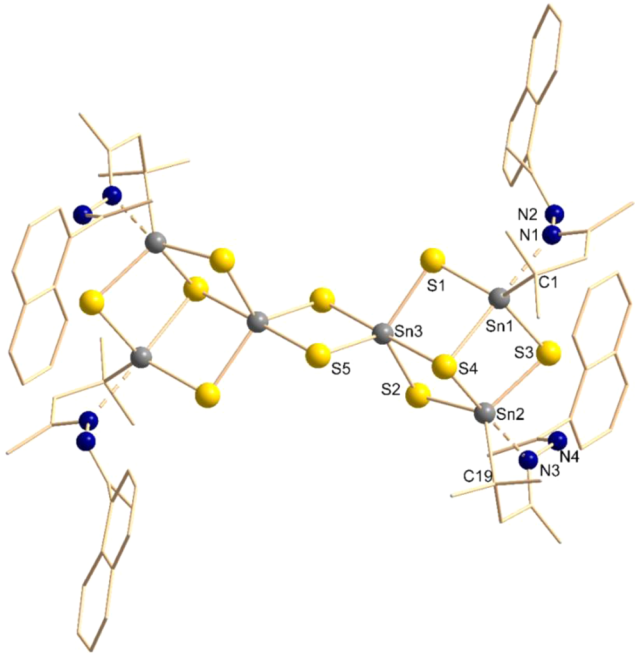

Figure 2. Molecular structure of the cluster in $7{\cdot}6CH_2Cl_2$. Thermal ellipsoids are shown with 50% probability, organic moieties are shown as wires, and H atoms are omitted for clarity. Atom color code: yellow, S; gray, Sn; blue, N.

Both of the two naphthyl groups at one defect-heterocubane unit, the planes of which include an angle of 45.16°, are oriented toward the same neighboring molecule. This results in self-complementary interactions between the respective aromatics, similar to common C−H···π interactions except for an unusual C−H−centroid angle. By continuation of the interactions through the other $[Sn_3S_4]$ moieties, one-dimensional zigzag chains are generated (Figure 3). The distances between the centroids of the six-membered rings and the H atoms of the next naphthyl molecule are relatively short and amount to 2.753 Å (A1···H) and 3.010 Å (A2···H).

The 2-(naphthalen-2-yl)ethylidene-substituted cluster was obtained with only one CH_2Cl_2 molecule per formula unit ($8{\cdot}CH_2Cl_2$), which resulted in a crystal structure with the triclinic space group $P\bar{1}$ (Figure 4). Regarding the structural parameters observed in the molecular structure (Table S2 in the Supporting Information), the deviation of the trans arrangements from ideal 180° angles is even smaller than that in $7{\cdot}6CH_2Cl_2$ (N1−Sn1−S4 177.66(9)°, N3−Sn2−S4 178.09(9)°, S4−Sn3−S5 179.39(3)°), whereas angles among Sn, N, and C atoms do not noticeably differ (C19−Sn2−N3 74.01(16)°, C1−Sn1−N1 76.26(15)°). The Sn−S distances range between 2.3798(17) (Sn3−S5′) and 2.8891(14) Å (Sn3−S4). The shortest and the longest Sn−S bonds are oriented cis at the same Sn atom (Sn3−S5′, Sn3−S4).

Adjacent molecules are arranged in a way that the naphthyl groups of one of the defect-heterocubane units of one cluster point between two naphthyl groups of an adjacent defect-heterocubane moiety from another cluster molecule. The alternating stacking of the four aromatic groups affords two nearly parallel orientations in the center with parallel-shifted

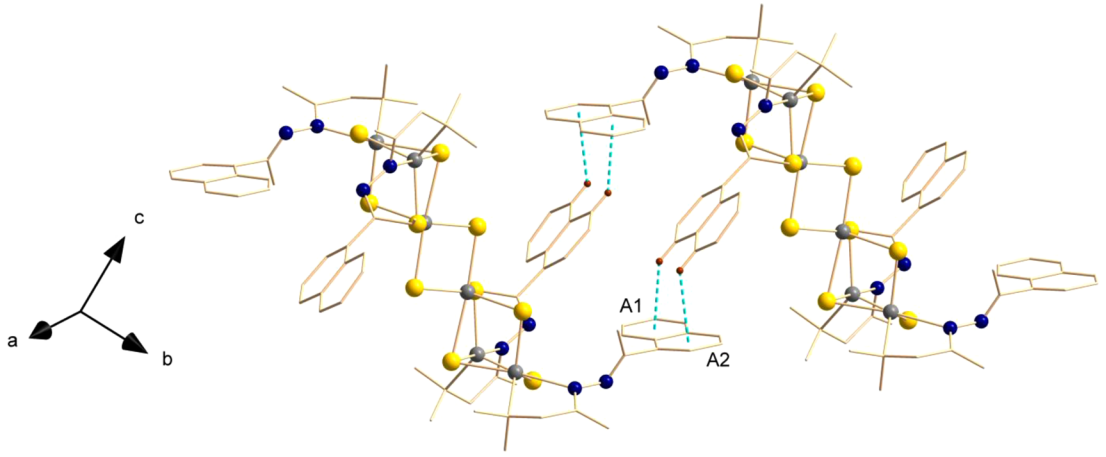

Figure 3. Packing of the cluster molecules in $7{\cdot}6CH_2Cl_2$. Organic moieties are shown as wires, and most of the H atoms and solvent molecules are omitted for clarity. Atom color code: yellow spheres, S; gray spheres, Sn; blue spheres, N; red spheres, H.

DOI: 10.1021/acs.organomet.5b00295
Organometallics XXXX, XXX, XXX−XXX

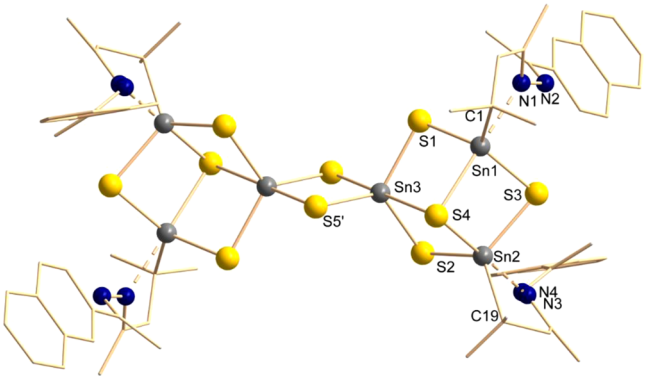

Figure 4. Molecular structure of the cluster in **8**·CH_2Cl_2. Thermal ellipsoids are shown with 50% probability, organic moieties are shown as wires, and H atoms are omitted for clarity. Atom color code: yellow, S; gray, Sn; blue, N.

face-to-face π-stacking interaction and two inclined orientations which resemble T-shaped π-stacking interactions (Figure 5). The first produces short distances of the aryl centroids (3.954 Å) and an angle of 23.67° between the ring normal and centroid contact axis. The H atom−centroid distances of the T-shaped π-stacking interactions are also typical: 3.123−3.730 Å.[16]

Our attempts to attach heteropolyaromatic groups to Sn/S clusters were successful for the decoration of an $[Sn_6S_{10}]$ cluster with a quinolin-6-ylmethyl-terminated ligand. Compound **10**·$2CH_2Cl_2$ crystallizes in the triclinic space group $P\bar{1}$. The molecular structure of the cluster molecule is shown in Figure 6.

Sn−S distances (Table S2 in the Supporting Information) vary between 2.3830(12) Å (Sn3−S5) and 2.7276(12) Å (Sn3−S4). According to the situation in **8**·CH_2Cl_2, the shortest and the longest Sn−S bonds share the same Sn atom. As usual, the longest bond (Sn3−S4) is found between the "inorganic" Sn atom (Sn3) and the μ_3-bridging sulfide ligand. The average Sn−(μ-S) bond length amounts to 2.41 Å, thus being situated those found in **7**·$6CH_2Cl_2$ and **8**·CH_2Cl_2. Sn−C distances (2.177(5) and 2.172(5) Å) and Sn−N distances (2.425(4) and 2.448(4) Å) are within the normal range. One observes a range of "linear" ligand arrangements around the organyl-bound Sn atoms (N1−Sn1−S4 178.09(10)°, N4−Sn2−S4 174.71(10)°) similar to that in **7**·$6CH_2Cl_2$. The intramolecular coordination of the azine N atoms to the Sn atoms includes distances of

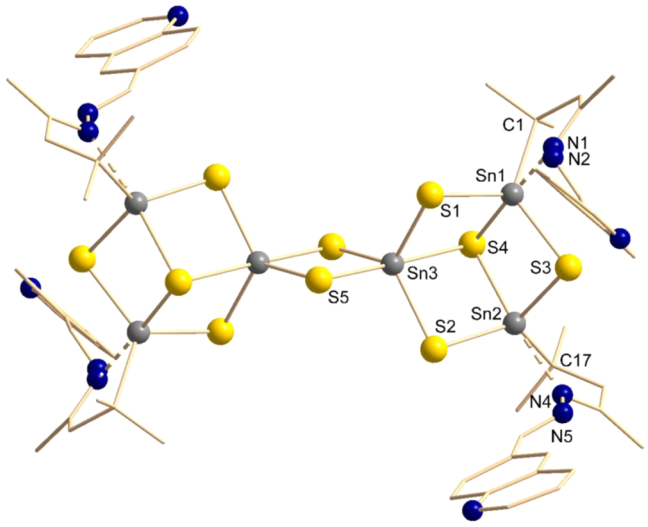

Figure 6. Molecular structure of the cluster in **10**·$2CH_2Cl_2$. Thermal ellipsoids are shown with 50% probability, organic moieties are shown as wires, and H atoms are omitted for clarity. Atom color code: yellow, S; gray, Sn; blue, N.

2.425(4) and 2.448(4) Å, thus being longer and therefore weaker than in the structures of **7** and **8**. This is in agreement with the different electronic properties of the aromatic systems, which include an electronegative heteroatom in **10** that withdraws electron density from the nearby azine group.

Similar to the crystal structures of **7** and **8**, four aromatic ligands from two $[Sn_3S_4]$ subunits of two adjacent cluster molecules are in close proximity, which reflects the similarities of the architectures of the organic ligand shell. As in **8**·CH_2Cl_2, two quinolinyl fragments meet in the center of the four-molecule arrangement in a parallel fashion, with an angle of 62.94° between their mean planes and those of the adjacent quinolone units. However, the arrangement in **10**·$2CH_2Cl_2$ only allows for the central, parallel-shifted face-to-face π-stacking interaction to occur, whereas a T-shaped π-stacking interaction with the outer ligand groups cannot be realized (Figure 7). Both distances and angles between the centroids in **10**·$2CH_2Cl_2$ correlate with characteristic interactions between two quinolines that possess electron-withdrawing substituents (Table 1).[17]

In the unit cells of **7**·$6CH_2Cl_2$ and **10**·$2CH_2Cl_2$ the cluster arrangements lead to the generation of alternating layers of

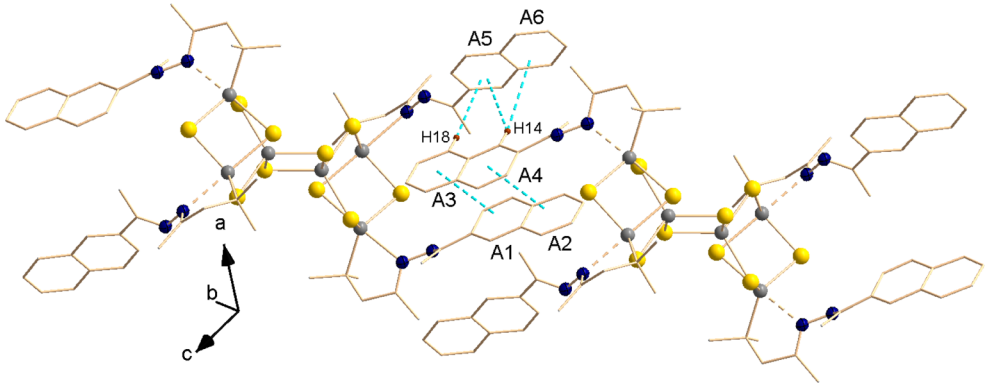

Figure 5. Packing of the cluster molecules in **8**·CH_2Cl_2. Organic moieties are shown as wires, and most of the H atoms and solvent molecules are omitted for clarity. Atom color code: yellow spheres, S; gray spheres, Sn; blue spheres, N; red spheres, H.

DOI: 10.1021/acs.organomet.5b00295
Organometallics XXXX, XXX, XXX−XXX

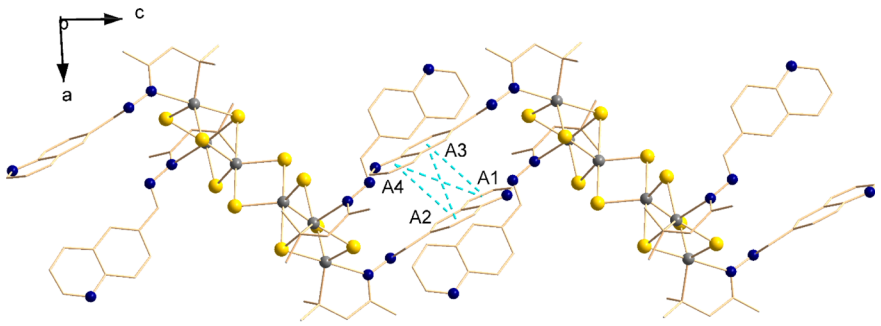

Figure 7. Packing of the cluster molecules in **10**·2CH_2Cl_2. Organic moieties are shown as wires, and H atoms and solvent molecules are omitted for clarity. Atom color code: yellow spheres, S; gray spheres, Sn; blue spheres, N; red spheres, H.

Table 1. Geometric Relations between the Ring Centroids or Ring Centroids and Adjacent H Atoms in 6, 7·6CH_2Cl_2, 8·CH_2Cl_2, and 9·2CH_2Cl_2[a]

Compound **6**				
	A1(A)···H10		A1(B)···H10	
distance (Å)	2.991		3.345	
$\alpha_\perp$ (deg)	12.17		12.09	
Compound 7·6CH_2Cl_2				
	A1···H		A2···H	
distance (Å)	2.753		3.010	
$\alpha_\perp$ (deg)	8.14		12.89	
Compound **8**·CH_2Cl_2				
	A1···A3	A2···A4	A5···H18,H14	A6···H14
distance (Å)	3.954	3.954	3.123, 3.408	3.730
$\alpha_\perp$ (deg)	22.06	25.85	30.53, 14.52	28.35
Compound **10**·2CH_2Cl_2				
	A1···A3	A1···A4	A2···A3	A2···A4
distance (Å)	3.926	5.045	4.103	3.926
$\alpha_\perp$ (deg)	25.97	45.49	30.83	25.97

[a]Distances are given between two ring centroids or between a ring centroid and an H atom, respectively. $\alpha_\perp$ is defined as either the angle between the ring normal of one ring and the centroid···centroid vector including a second ring or the angle between the plane defined by a ring and the corresponding H atom···ring centroid vector.

inorganic and organic components of the molecules. The solvent molecules are incorporated between the inorganic units. Geometric relations between the ring centroids that are involved in the diverse interactions in 7·6CH_2Cl_2, **8**·CH_2Cl_2, and **10**·2CH_2Cl_2 are summarized in Table 1.

CONCLUSION

A straightforward method for the conversion of diverse aromatic molecules into their hydrazone derivatives was found that does not require working under inert conditions. The connection of the aromatic molecules with Sn/S clusters was possible in all cases, which was proven by means of single-crystal X-ray diffraction studies or by mass spectrometry. The crystallization tendency of the ligand-decorated Sn/S clusters seems to decrease with increasing size of the aromatic molecules. In the crystal structures, polyaromatic ligands are involved in notable intramolecular and intermolecular π-stacking interactions, in agreement with the behavior of such systems in other contexts. Future work will focus on the interaction of metal atoms and ions with the aromatic rings.

EXPERIMENTAL SECTION

Syntheses. We describe herein a mild and straightforward method to convert aromatic aldehydes or ketones to their hydrazine derivative according to the following general procedure, which combined methods reported previously by Lee[18] and Wyles.[19] Our approach was similar to the synthesis procedure by Wyles and similar to the workup procedure described by Lee: 20 mg of the substrate was dissolved in 20 mL of ethanol. A ! mL portion of hydrazine hydrate (80% in water) was added, and the mixture was heated to reflux for *x* hours (for the value of *x*, see below). The solution was then stirred at room temperature for 12 h and extracted several times with chloroform to give a slightly yellow solution, until the chloroform phase remained colorless. The organic phases were combined, dried over $MgSO_4$, filtered, and evaporated. The resulting residue was analyzed by means of mass spectrometry and/or NMR spectroscopy. Yields are 44−100% (see below). All molecules are depicted in Scheme 2. New compounds are denoted by Arabic numbers.

Benzaldehyde Hydrazone. x = 1. Yield: 14 mg (1.21×10^{-4} mol, 64%), yellow oil. ^{1}H NMR (300.1 MHz, $CDCl_3$): δ 8.68 (s, 1H), 7.90−7.81 (m, 2H). 7.50−7.44 (m, 3H), 5.54 (s, 2H, NH_2) ppm.

1-Acetonaphthone Hydrazone. x = 2.5. Yield: 17 mg (9.28×10^{-5} mol, 79%), yellow solid. ^{1}H NMR (300.1 MHz, C_7D_8): δ 8.29−8.19 (m, 2H, *E*+*Z*), 7.63−7.55 (m, 1H, *E*+*Z*), 7.55−7.48 (m, 1H, *E*+*Z*), 7.34−7.13 (m, 4H, *E*+*Z*), 4.79 (s, 2H, NH_2, *E*/*Z*), 4.49 (s, 2H, NH_2, *E*/*Z*), 2.18 (s, 3H, *E*/*Z*), 1.73 (s, 3H, *E*/*Z*) ppm. ESI$^+$-MS: calculated 185.1073 $[M + H]^+$, found 185.1077. The molecule shows *E*/*Z* isomerism in solution, to be reflected in the NMR spectrum.

2-Acetonaphthone Hydrazone. x = 3. Yield: 9 mg (5.17×10^{-5} mol, 44%), yellow solid. ^{1}H NMR (300.1 MHz, C_7D_8): δ 8.33−8.25 (m, 2H, *E*+*Z*), 8.17−8.10 (m, 2H, *E*+*Z*), 7.97−7.82 (m, 6H, *E*+*Z*), 7.62−7.49 (m, 2H, *E*+*Z*), 2.52 (s, 3H, *E*/*Z*), 2.47 (s, 3H, *E*/*Z*) ppm. ESI$^+$-MS: calculated 185.1073 $[M + H]^+$, found 185.1070. The molecule shows *E*/*Z* isomerism in solution, to be reflected in the NMR spectrum.

Quinoline-3-carbaldehyde Hydrazone. x = 4. Yield: 21 mg (1.27×10^{-4} mol, quantitative), yellow solid. ^{1}H NMR (300.1 MHz, $CDCl_3$): δ 9.20 (d, 1H, ^3J = 1.89 Hz), 8.10 (d, 1H, ^3J = 1.86 Hz), 8.08 (d, 1H, ^2J = 8.48 Hz), 7.86 (s, 1H), 7.78 (d, 1H, ^2J = 7.95 Hz), 7.67 (ddd, 1H, ^2J = 7.67 Hz, ^3J = 1.24 Hz), 7.52 (ddd, 1H, ^2J = 7.46 Hz, ^3J = 0.93 Hz), 5.76 (s, 2H, NH_2) ppm. ESI$^+$-MS: calculated 172.0869 $[M + H]^+$, found 172.0867.

*Quinoline-6-carbaldehyd4 Hydrazone (**1**).* x = 4. Yield: 21 mg (1.27×10^{-4} mol, quantitative), yellow solid. ^{1}H NMR (300.1 MHz, $CDCl_3$): δ 8.87 (dd, 1H, ^2J = 4.30 Hz, ^3J = 1.65 Hz), 8.12 (dd, 1H, ^2J = 8.30 Hz, ^3J = 1.46 Hz), 8.06 (s, 2H), 7.89 (s, 1H), 7.78 (s, 1H), 5.70 (s, 2H, NH_2) ppm. ESI$^+$-MS: calculated 172.0869 $[M + H]^+$, found 172.0867.

*3-Acetylquinoline Hydrazone (**2**).* x = 4. Yield: 16 mg (8.64×10^{-5} mol, 74%) yellow solid. ^{1}H NMR (300.1 MHz, $CDCl_3$): δ 9.37 (d, 1H, ^3J = 2.28 Hz), 8.18 (s, 1H), 8.10 (d, 1H, ^2J = 8.49 Hz), 7.80 (d, 1H, ^2J = 8.13 Hz), 7.67 (dd, 1H, ^2J = 7.55 Hz, ^3J = 1.39 Hz), 7.52 (dd, 1H, ^2J = 7.46 Hz, ^3J = 1.41 Hz), 5.50 (s, 2H, NH_2), 2.21 (s, 3H) ppm. ESI$^+$-MS: calculated 186.1026 $[M + H]^+$, found 186.1023.

DOI: 10.1021/acs.organomet.5b00295
Organometallics XXXX, XXX, XXX−XXX

Scheme 2. Aromatic Hydrazones Derived from the Corresponding Aldehydes or Ketones

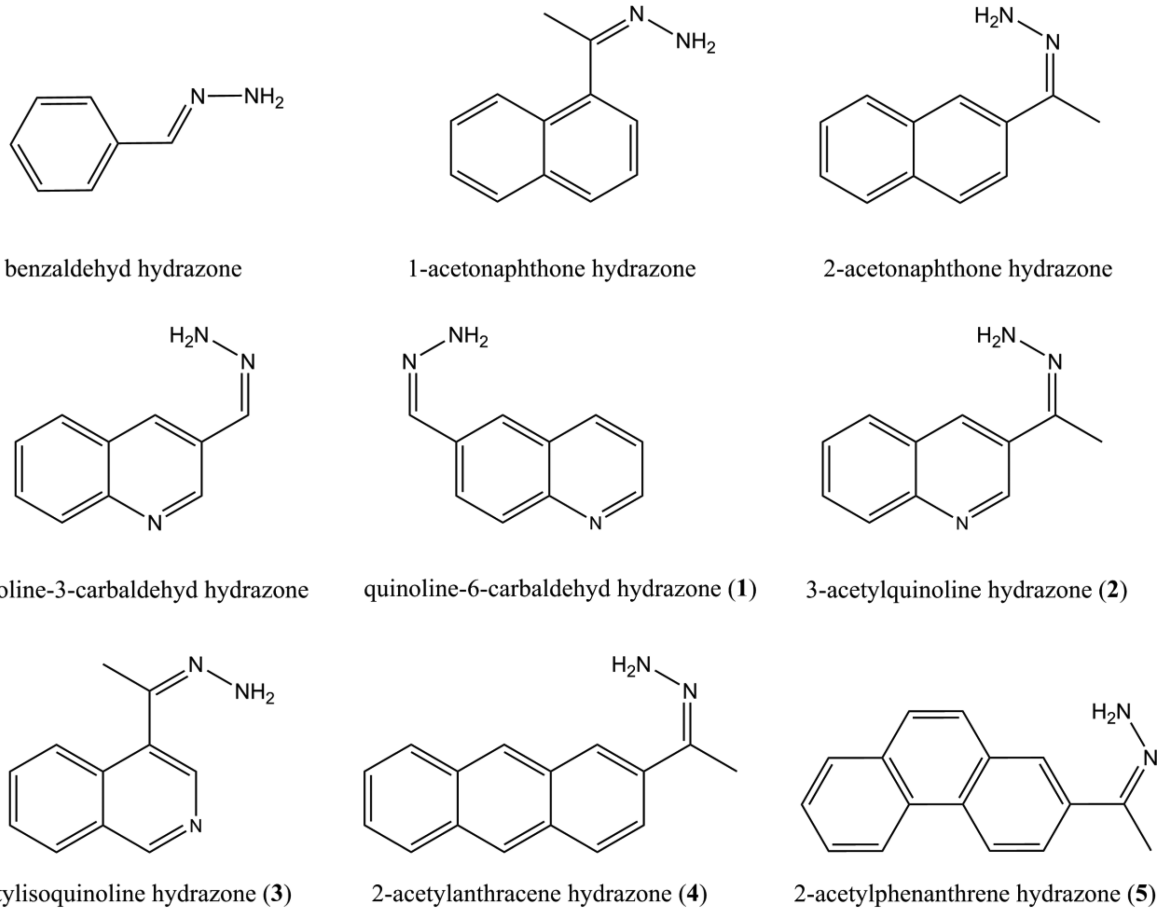

Scheme 3. Synthesis and Structure Diagram of $[(R^1Sn)_4S_6]$ (A; $R^1 = -CMe_2CH_2C(O)Me$)

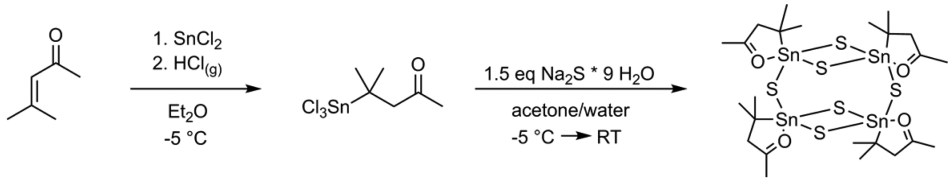

*4-Acetylisoquinoline Hydrazone (**3**).* x = 4. Yield: 21 mg (1.17×10^{-4} mol, quantitative), yellow solid. ^{1}H NMR (300.1 MHz, $CDCl_3$): δ 9.18 (s, 1H), 8.49 (s, 1H), 8.23 (d, 1H, ^2J = 8.40 Hz), 7.98 (d, 1H, ^2J = 8.07 Hz), 7.80−7.56 (m, 2H), 4.97 (s, 2H, NH_2), 2.30 (s, 3H) ppm. ESI$^+$-MS: calculated 186.1026 $[M + H]^+$, found 186.1025.

*2-Acetylanthracene Hydrazone (**4**).* x = 3. Yield: 11 mg (4.54×10^{-5} mol, 50%), golden plates. ^{1}H NMR (300.1 MHz, C_7D_8): δ 8.38 (dd, 1H, ^2J = 9.09 Hz, ^3J = 1.50 Hz), 8.09 (s, 1H), 8.04 (s, 1H), 7.80−7.70 (m, 4H), 7.28−7.18 (m, 2H), 4.83 (s, 2H, NH_2), 1.71 (s, 3H) ppm. The molecule shows E/Z isomerism in solution, to be reflected in the NMR spectrum. The signals of E and Z isomers are superposed on each other in a way that inhibits a discrimination between E and Z conformations.

*2-Acetylphenanthrene Hydrazone (**5**).* x = 3. Yield: 19 mg (8.26×10^{-5} mol, 91%), cream-colored solid. ^{1}H NMR (300.1 MHz, C_7D_8): δ 8.90−8.82 (m, 1H, E+Z), 8.60−8.54 (m, 1H, E+Z), 8.15−8.07 (m, 1H, E+Z), 7.66−7.56 (m, 2H, E+Z), 7.47−7.44 (m, 2H, E+Z), 7.43−7.31 (m, 2H, E+Z), 4.83 (s, 2H, NH_2, E+Z), 1.72 (s, 3H, E/Z), 1.71 (s, 3H, E/Z) ppm. The molecule shows E/Z isomerism in solution, to be reflected in the NMR spectrum.

The organo-functionalized Sn/S cluster $[(R^1Sn)_4S_6]$ (**A**) was prepared according to the literature procedure (see Scheme 3).[4,5]

Subsequent reactions of the hydrazones/hydrazines with **A** were realized according to the following general procedure under strict exclusion of external moisture and oxygen, using standard Schlenk-line techniques or an Ar atmosphere with a glovebox: 1.0 equiv of **A** (30 mg, 2.82×10^{-5} mol) and 4.4 equiv of the corresponding hydrazone/hydrazide were evacuated for 30 min and then flowed with argon and suspended in 8 mL of CH_2Cl_2. The suspension was stirred for some time x, filtered, and layered with solvent y. After a certain time z, the solution and/or the crystals were analyzed via electrospray ionization mass spectrometry (ESI-MS) and/or EDX and/or single crystal X-ray diffraction (for x, y, and z, see below). Images of the high-resolution mass spectra (HRMS) of those compounds that have not been obtained as single crystals are given in the Supporting Information (Figures S1−S6). Single-crystal yields amount to ca. 25−35% with respect to the starting material, increasing with a decreasing number of aromatic rings, as discussed below. The identity and purity of the bulk material was confirmed via mass spectrometry. All NMR spectra—except that of compound **10**—were recorded on reaction solutions due to the relatively low yields and poor solubility of the compounds; therefore, a discrimination between the signals of defect-heterocubane cluster cations and the doubly μ-S bridged "dimeric" clusters was not possible; the ^{1}H NMR spectra additionally show the signals of further byproducts that could not be identified. Figure S8 in the Supporting

DOI: 10.1021/acs.organomet.5b00295
Organometallics XXXX, XXX, XXX−XXX

Information shows the ^{1}H and ^{119}Sn NMR spectra of compound **10**, which was measured on a solution of single crystals.

*Synthesis of [(C_6H_5CH═NN═$CMeCH_2CMe_2$)$_2Sn_3S_4$(μ-S)]$_2$ (**6**) by Reaction of **A** with Benzaldehyde Hydrazone.* *x*, *y*, *z*: 2 days, *n*-hexane, 6 weeks; colorless crystals. MS (ESI$^+$): *m*/*z* (%) 1087.1 (32) [$(C_{13}H_{17}N_2Sn)_3S_4$]$^+$; 1834.8 (16). HRMS (ESI$^+$): *m*/*z* calcd 1089.0125 [$(C_{13}H_{17}N_2Sn)_3S_4$]$^+$, found 1089.0112. ^{1}H NMR (300 MHz, CD_2Cl_2): δ 8.70 (1H, H_{Azine}), 7.92−7.01 (m, 5H, H_{Ar}), 2.25−2.12 (m, 2H, CH_2), 1.41 (s, 6H, CMe_2), 1.34 (s, 3H, CMe) ppm. ^{119}Sn NMR (112 MHz): δ −48, −75 ppm.

*Synthesis of [($C_{10}H_7CMe$═NN═$CMeCH_2CMe_2$)$_2Sn_3S_4$(μ-S)]$_2$·6CH_2Cl_2 (**7**·6CH_2Cl_2) by Reaction of **A** with 1-Acetonaphthone Hydrazone.* *x*, *y*,*z*: 8 days, Et_2O, 3 weeks; colorless crystals. MS (ESI$^+$): *m*/*z* (%) 1281.3 (100) [$(C_{18}H_{21}N_2Sn)_3S_4$]$^+$. HRMS (ESI$^+$): *m*/*z* calcd 1279.1065 [$(C_{18}H_{21}N_2Sn)_3S_4$]$^+$; found 1279.1063. ^{1}H NMR (300 MHz, CD_2Cl_2): δ 8.00−7.00 (m, 7H, H_{Ar}), 2.87 (s, 2H, CH_2), 2.39 (s, 3H, CMe), 2.29 (s, 6H, CMe_2) ppm. ^{119}Sn NMR (112 MHz): δ −63, −87 ppm.

*Synthesis of [($C_{10}H_7CMe$═NN═$CMeCH_2CMe_2$)$_2Sn_3S_4$(μ-S)]$_2$·CH_2Cl_2 (**8**·CH_2Cl_2) by Reaction of **A** with 2-Acetonaphthone Hydrazone.* *x*, *y*, *z*: 2 days, toluene, 3 weeks; colorless crystals. MS (ESI$^+$): *m*/*z* (%) 963.3 (49), 999.6 (8), 1077.6 (33), 1528.0 (29). None of the signals concur with the structure that was verified by single-crystal X-ray diffraction. This indicates decomposition either in solution or under the measurement conditions. EDX: Sn/S calcd 6:10, found 5.55:10. ^{1}H NMR (300 MHz, CD_2Cl_2): δ 7.97−7.79 (m, 5 H, H_{Ar}), 7.63−7.45 (m, 3H, H_{Ar}), 2.53 (s, 2H, CH_2), 2.38 (s, 3H, Me), 2.26 (s, 6H, CMe_2), 2.15 (s, 3H, Me) ppm. ^{119}Sn NMR (112 MHz): δ −67 ppm.

*Synthesis of [(C_9H_8CMe═NN═$CMeCH_2CMe_2$)$_2Sn_3S_4$(μ-S)]$_2$ (**9**) by Reaction of **A** with 3-Quinolinecarbaldehyde Hydrazone.* *x*, *y*, *z*: 4 days, Et_2O, toluene, *n*-hexane; no crystalline products. MS (ESI$^+$): *m*/*z* (%) 438.2 (25), 841.2 (5), 962.1 (10), 1101.2 (30), 1240.2 (77) [$(C_{16}H_{18}N_3Sn)_3S_4$]$^+$; 1676.5 (8). HRMS (ESI$^+$): *m*/*z* calcd 1240.0451 [$(C_{16}H_{18}N_3Sn)_3S_4$]$^+$, found 1240.0446 (Figure S1 in the Supporting Information). Although the mass spectrum only shows the [$(C_{16}H_{18}N_3Sn)_3S_4$]$^+$ species, we assume the formation of the quoted cluster with two doubly μ-S bridged defect-heterocubane units as the main product. This assumption is based on the fact that compounds **6**−**8** and **10** show the same behavior in ESI(+) mass spectrometry. ^{1}H NMR (300 MHz, CD_2Cl_2): δ 8.16−7.55 (m, H_{Ar}), 2.31−2.26 (m, 8H, CH2, CMe_2), 2.20 (3H, CMe), 2.10 (3H, CMe) ppm. ^{119}Sn NMR (112 MHz, CD_2Cl_2): δ −72 ppm.

*Synthesis of [(C_9H_8NCH═NN═$CMeCH_2CMe_2$)$_2Sn_3S_4$(μ-S)]$_2$·2CH_2Cl_2 (**10**·2CH_2Cl_2) by Reaction of **A** with 6-Quinolinecarbaldehyde Hydrazone (**1**).* *x*, *y*, *z*: 4 days, Et_2O, 2 weeks; red crystals. MS (ESI$^+$): *m*/*z* (%) 438.2 (28), 839.2 (5), 1087.2 (8), 1240.3 (77) [$(C_{16}H_{18}N_3Sn)_3S_4$]$^+$. HRMS (ESI$^+$): *m*/*z* calcd 1240.0451 [$(C_{16}H_{18}N_3Sn)_3S_4$]$^+$, found 1240.0453. ^{1}H NMR (300 MHz, CD_2Cl_2): δ 9.51 (s, 1H, $H_{Hydrazone}$), 8.26−7.15 (m, H_{Ar}), 2.77 (s, 2H, CH_2), 2.29 (s, 3H, C_{Me}), 1.50 (s, 6H, CMe_2) ppm (Figure S8, top, in the Supporting Information). ^{119}Sn NMR (112 MHz, CD_2Cl_2): δ −48, −73 ppm (Figure S8, bottom).

*Synthesis of [(C_9H_6NCMe═NN═$CMeCH_2CMe_2$)$_2Sn_3S_4$(μ-S)]$_2$ (**11**) by Reaction of **A** with 3-Acetylquinoline Hydrazone (**2**).* *x*, *y*, *z*: 5 days, toluene, thf, Et_2O; no crystalline products. MS (ESI$^+$): *m*/*z* (%) 1282.5 (100) [$(C_{17}H_{20}N_3Sn)_3S_4$]$^+$. HRMS (ESI$^+$): *m*/*z* calcd 1282.0918 [$(C_{17}H_{20}N_3Sn)_3S_4$]$^+$, found 1282.0918 (Figure S2 in the Supporting Information). Although the mass spectrum only shows the [$(C_{17}H_{20}N_3Sn)_3S_4$]$^+$ species, we assume the formation of the quoted cluster with two doubly μ-S bridged defect-heterocubane units as the main product. This assumption is based on the fact that compounds **6**−**8** and **10** show the same behavior in ESI(+) mass spectrometry. ^{1}H NMR (300 MHz, CD_2Cl_2): δ 8.09−7.52 (m, H_{Ar}), 2.39 (s, 2H, CH_2), 2.25 (s, 6H, CMe_2), 2.16 (s, 3H, CMe), 1.94 (s, 3H, CMe) ppm. ^{119}Sn NMR (112 MHz, CD_2Cl_2): δ −58 ppm.

*Synthesis of [(C_9H_6NCMe═NN═$CMeCH_2CMe_2$)$_2Sn_3S_4$(μ-S)]$_2$ (**12**) by Reaction of **A** with 4-Acetylisoquinoline Hydrazone (**3**).* *x*, *y*, *z*: 1 day, Et_2O, EtOH, *n*-hexane; no crystalline products. MS (ESI$^+$): *m*/*z* (%) 1284.2 (100) [$(C_{17}H_{20}N_3Sn)_3S_4$]$^+$. HRMS (ESI$^+$): *m*/*z* calcd 1282.0918 [$(C_{17}H_{20}N_3Sn)_3S_4$]$^+$, found 1282.0929 (Figure S3 in the Supporting Information). Although the mass spectrum only shows the [$(C_{17}H_{20}N_3Sn)_3S_4$]$^+$ species, we assume the formation of the quoted cluster with two doubly μ-S bridged defect-heterocubane units as the main product. This assumption is based on the fact that compounds **6**−**8** and **10** show the same behavior in ESI(+) mass spectrometry. ^{1}H NMR (300 MHz, CD_2Cl_2): δ 7.78−7.63 (m, H_{Ar}), 2.36 (s, 2H, CH_2), 2.31 (s, 6H, CMe_2), 2.16 (s, 3H, CMe), 1.96 (s, 3H, CMe) ppm. ^{119}Sn NMR (112 MHz, CD_2Cl_2): δ −61 ppm.

*Synthesis of [($C_{14}H_9CMe$═NN═$CMeCH_2CMe_2$)$_2Sn_3S_4$(μ-S)]$_2$ (**13**) by Reaction of **A** with 2-Acetylanthracene Hydrazone (**4**).* *x*, *y*, *z*: 1 day or 2 days, Et_2O, EtOH, *n*-hexane, toluene, thf; no crystalline products. MS (ESI$^+$): *m*/*z* (%) 1215.3 (18), 1429.4 (100) [$(C_{22}H_{23}N_2Sn)_3S_4$]$^+$. HRMS (ESI$^+$): *m*/*z* calcd 1431.1544 [$(C_{22}H_{23}N_2Sn)_3S_4$]$^+$, found 1431.1514 (Figure S4 in the Supporting Information). Although the mass spectrum only shows the [$(C_{22}H_{23}N_2Sn)_3S_4$]$^+$ species, we assume the formation of the quoted cluster with two doubly μ-S bridged defect-heterocubane units as the main product. This assumption is based on the fact that compounds **6**−**8** and **10** show the same behavior in ESI(+) mass spectrometry. ^{1}H NMR (300 MHz, CD_2Cl_2): δ 8.71−7.53 (m, H_{Ar}), 2.78 (s, 2H, CH_2), 2.16 (s, 3H, CMe), 2.14 (s, 3H, CMe), 1.91 (s, 6H, CMe) ppm. ^{119}Sn NMR (112 MHz, CD_2Cl_2): δ −62 ppm.

*Synthesis of [($C_{14}H_9CMe$═NN═$CMeCH_2CMe_2$)$_2Sn_3S_4$(μ-S)]$_2$ (**14**) by Reaction of **A** with 2-Acetylphenanthrene Hydrazone (**5**).* *x*, *y*, *z*: 1 day in the dark, Et_2O, EtOH, *n*-hexane; no crystalline products. MS (ESI$^+$): *m*/*z* (%) 1215.4 (37), 1431.4 (100) [$(C_{22}H_{23}N_2Sn)_3S_4$]$^+$. HRMS (ESI$^+$): *m*/*z* calcd 1431.1541 [$(C_{22}H_{23}N_2Sn)_3S_4$]$^+$, found 1431.1498 (Figure S5 in the Supporting Information). Although the mass spectrum only shows the [$(C_{22}H_{23}N_2Sn)_3S_4$]$^+$ species, we assume the formation of the quoted cluster with two doubly μ-S bridged defect-heterocubane units as the main product. This assumption is based on the fact that compounds **6**−**8** and **10** show the same behavior in ESI(+) mass spectrometry. ^{1}H NMR (300 MHz, CD_2Cl_2): δ 7.85−7.17 (m, 7H, H_{Ar}), 2.47 (s, 2H, CH_2), 2.36 (s, 3H, Me), 2.15 (s, 3H, Me), 2.02 (s, 3H, Me), 1.83 (s, 3, Me) ppm. ^{119}Sn NMR (112 MHz): δ −61 ppm.

*Synthesis of [($C_{10}H_7NHN$═$CMeCH_2CMe_2$)$_2Sn_3S_4$(μ-S)]$_2$ (**15**) by Reaction of **A** with 1-Naphthylhydrazine.* A 0.17 mmol portion of 1-naphthylhydrazine hydrochloride was suspended in 5 mL of water, and a saturated solution of sodium hydrogen carbonate was added until the suspension became basic. Solvent was then removed in vacuo, and the resulting residue was dried for 30 min under vacuum. It was dissolved in 7 mL of CH_2Cl_2 and a solution of 0.038 mmol of **A** in 4 mL of CH_2Cl_2 was added. Filtration after 6 days and subsequent layering with toluene or thf, respectively, did not yield crystalline products. MS (ESI$^+$): *m*/*z* (%) 541.1 (13), 671.2 (13), 722.8 (15), 822.9 (10), 964.9 (10), 1061.1 (36), 1201.1 (100) [$(C_{16}H_{20}N_2Sn)_3S_4$]$^+$. HRMS (ESI$^+$): *m*/*z* calcd 1201.0594 [$(C_{16}H_{20}N_2Sn)_3S_4$]$^+$, found 1201.0616 (Figure S6 in the Supporting Information). Although the mass spectrum only shows the [$(C_{16}H_{20}N_2Sn)_3S_4$]$^+$ species, we assume the formation of the quoted cluster with two doubly μ-S bridged defect-heterocubane units as the main product. This assumption is based on the fact that compounds **6**−**8** and **10** show the same behavior in ESI(+) mass spectrometry. ^{1}H NMR (300 MHz, CD_2Cl_2): δ 7.90−7.72 (m, 3H, H_{Ar}), 7.52−7.27 (m, 4H, H_{Ar}), 2.88 (s, 2H, CH_2), 1.89 (s, 3H, Me), 1.81 (s, 3H, Me) ppm. ^{119}Sn NMR (112 MHz): δ −69, −81 ppm.

Single-Crystal X-ray Diffraction Analyses. Data were collected on a diffractometer equipped with an STOE imaging plate detector system IPDS2 or 2T or a Bruker D8 Quest instrument, using Mo Kα radiation with graphite monochromatization (λ 0.71073 Å) at 100 K. The structure solution was performed using direct methods, full-matrix least-squares refinement against F^2, with SHELXTL software and the OLEX2 software package.[20,21] Details of the data collections and refinements are given in Table S1 (see the Supporting Inforamtion). Structural data of all compounds are summarized in Table S2 (see the Supporting Inforamtion).

Spectroscopy and Spectrometry. ^{1}H NMR, ^{13}C NMR, and ^{119}Sn NMR measurements were carried out using Bruker DRX 300 and 400 MHz spectrometers at 25 °C. In ^{1}H and ^{13}C NMR spectra, chemical shifts are quoted in ppm relative to the residual protons of

DOI: 10.1021/acs.organomet.5b00295
Organometallics XXXX, XXX, XXX−XXX

deuterated solvents. For ^{119}Sn NMR measurements, Me_4Sn was used as an internal standard. Mass spectrometry (MS) was performed on a Finnigan MAT 95S isntrument. Electrospray ionization mass spectrometry (ESI-MS) was performed on a Finnigan LTQ-FT spectrometer by Thermo Fischer Scientific in the positive ion mode with solvent as carrier gas. EDX analysis was performed using the EDX device Voyager 4.0 of Noran Instruments coupled with a CamScan CS 4DV electron microscope. Data acquisition was performed with an acceleration voltage of 20 kV and 100 s accumulation time. For the analysis, multiple single crystals were used and the data were recorded for both various times on a single crystal and various times on other single crystals.

■ ASSOCIATED CONTENT

Supporting Information

Figures, tables, and CIF files giving mass spectra and structure diagrams of compounds **9** and **11**−**15** and crystallographic tables and a supplementary crystallographic figure. The Supporting Information is available free of charge on the ACS Publications website at DOI: 10.1021/acs.organomet.5b00295.

■ AUTHOR INFORMATION

Corresponding Author

*S.D.: fax, +49 6421 2825653; tel, +49 6421 2825751; e-mail, dehnen@chemie.uni-marburg.de.

Notes

The authors declare no competing financial interest.

■ ACKNOWLEDGMENTS

This work was supported by the Deutsche Forschungsgemeinschaft (DFG) within the framework of GRK1782. We thank Jan Christmann for his help with the syntheses and NMR spectroscopic characterization of the title compounds.

■ REFERENCES

(1) (a) Fuhr, O.; Dehnen, S.; Fenske, D. *Chem. Soc. Rev.* **2013**, *42*, 1871−1906. (b) Maity, P.; Tsunoyama, H.; Yamauchi, M.; Xie, S.; Tsukuda, T. *J. Am. Chem. Soc.* **2011**, *133*, 20123−20125. (c) Aoki, K.; Chen, J.; Yang, N.; Nagasawa, H. *Langmuir* **2003**, *19*, 9904−9909.

(2) (a) Raynal, M.; Ballester, P.; Vidal-Ferran, A.; van Leeuwen, P. W. N. M. *Chem. Soc. Rev.* **2014**, *43*, 1660−1733. (b) Xu, W.; Jiang, F.; Zhou, Y.; Xiong, K.; Chen, L.; Yang, M.; Feng, R.; Hong, M. *Dalton Trans.* **2012**, *41*, 7737−7745. (c) Zhou, C.; Li, Y. *J. Colloid Interface Sci.* **2013**, *397*, 45−64. (d) Wang, L.-M.; Fan, Y.; Wang, Y.; Xiao, L.-N.; Hu, Y.-Y.; Peng, Y.; Wang, T.-G.; Gao, Z.-M.; Zheng, D.-F.; Cui, X.-B.; Xu, J.-Q. *J. Solid Sate Chem.* **2012**, *191*, 257−262.

(3) (a) Suga, S.; Manabe, T.; Yoshida, J. *Chem. Commun.* **1999**, 1237−1238. (b) Clive, D.; Yang, W. *J. Org. Chem.* **1995**, *60*, 2607−2609. (c) Tagne Kuate, A.; Iovkova, L.; Hiller, W.; Schürmann, M.; Jurkschat, K. *Organometallics* **2010**, *29*, 5456−5471. (d) Pabst, G.; Pfüller, O.; Sauer, J. *Tetrahedron* **1999**, *55*, 5047−5066. (e) Barbul, I.; Varga, R. A.; Molloy, K. C.; Silvestru, C. *Dalton Trans.* **2013**, *42*, 15427−15436.

(4) (a) Hassanzadeh Fard, Z.; Müller, C.; Harmening, T.; Pöttgen, R.; Dehnen, S. *Angew. Chem., Int. Ed.* **2009**, *48*, 4441−4444.

(5) (a) Hassanzadeh Fard, Z.; Clérac, R.; Dehnen, S. *Chem. - Eur. J.* **2010**, *16*, 2050−2053. (b) Hassanzadeh Fard, Z.; Hołyńska, M.; Dehnen, S. *Inorg. Chem.* **2010**, *49*, 5748−5752. (c) Halvagar, M. R.; Hassanzadeh Fard, Z.; Dehnen, S. *Chem. Commun.* **2010**, *46*, 4716−4718. (d) Fard, Z. H.; Halvagar, M. R.; Dehnen, S. *J. Am. Chem. Soc.* **2010**, *132*, 2848−2849. (e) Halvagar, M. R.; Hassanzadeh Fard, Z.; Dehnen, S. *Chem. - Eur. J.* **2011**, *17*, 4371−4374.

(6) Hutton, R. E.; Burley, J. W.; Oakes, V. *J. Organomet. Chem.* **1978**, *156*, 369−382.

(7) (a) Ipe, B. I.; Yoosaf, K.; Thomas, K. G. *J. Am. Chem. Soc.* **2006**, *128*, 1907−1913. (b) O'Regan, K. G.; Grätzel, M. *Nature* **1991**, *353*, 737−740. (c) Maeda, H.; Sakamoto, R.; Nishimori, Y.; Sendo, J.; Toshimitsu, F.; Yamanoi, Y.; Nishihara, H. *Chem. Commun.* **2011**, *47*, 8644−8646.

(8) Barth, B. E. K.; Leusmann, E.; Harms, K.; Dehnen, S. *Chem. Commun.* **2013**, *49*, 6590−6592.

(9) (a) You, Z.; Dehnen, S. *Inorg. Chem.* **2013**, *52*, 12332−12334. (b) Leusmann, E.; Wagner, M.; Rosemann, N. W.; Chatterjee, S.; Dehnen, S. *Inorg. Chem.* **2014**, *53*, 4228−4233.

(10) Liu, Y.; Najafabadi, B. K.; Fard, M. A.; Corrigan, J. F. *Angew. Chem., Int. Ed.* **2015**, *54*, 1−5.

(11) Adams, R. D.; Qu, B.; Smith, M. D. *Organometallics* **2002**, *21*, 4847−4852.

(12) (a) Chandrasekhar, V.; Nagendran, S.; Bansal, S.; Kozee, M. A.; Powell, D. R. *Angew. Chem., Int. Ed.* **2000**, *39*, 1833−1835. (b) Chandrasekhar, V.; Nagendran, S.; Bansal, S.; Cordes, A. W.; Vij, A. *Organometallics* **2002**, *21*, 3297−3300. (c) Chandrasekhar, V.; Gopal, K.; Nagendran, S.; Singh, P.; Steiner, A.; Zacchini, S.; Bickley, J. F. *Chem. - Eur. J.* **2005**, *11*, 5437−5448. (d) Zheng, G.-L.; Ma, J.-F.; Su, Z.-M.; Yan, L.-K.; Yang, J.; Li, Y.-Y.; Liu, J.-F. *Angew. Chem., Int. Ed.* **2004**, *43*, 2409−2411.

(13) Balch, A. L.; Olmstead, M. M. *Chem. Rev.* **1998**, *98*, 2123−2165.

(14) (a) Mancilla, T.; Carrillo, L.; Rivera, L. S. Z.; Camacho, C. C.; de Vos, D.; Kiss, R.; Darro, F.; Mahieu, B.; Tiekink, E. R. T.; Rahier, H.; Gielen, M.; Kemmer, M.; Biesemans, M.; Willem, R. *Appl. Organomet. Chem.* **2001**, *15*, 593−603. (b) Varga, R. A.; Jurkschat, K.; Silvestru, C. *Eur. J. Inorg. Chem.* **2008**, 708−716. (c) Vafaee, M.; Amini, M. M.; Khavasi, H. R.; Ng, S. W.; Tiekink, E. R. T. *Appl. Organomet. Chem.* **2012**, *26*, 471−477. (d) Novák, M.; Dostál, L.; Růžička, A.; Jambor, R. *Inorg. Chim. Acta* **2014**, *410*, 20−28.

(15) Hassanzadeh Fard, Z.; Xiong, L.; Müller, C.; Hołyńska, M.; Dehnen, S. *Chem. - Eur. J.* **2009**, *15*, 6595−6604.

(16) Hunter, A.; Thornton, J. M.; Singh, J. *J. Mol. Biol.* **1991**, *218*, 837−846.

(17) Janiak, C. *J. Chem. Soc. Dalton Trans.* **2000**, 3885−3896.

(18) Lee, K.-J.; Kim, J. L.; Hong, M. K.; Lee, J. Y. *J. Heterocycl. Chem.* **1999**, *36*, 1235−1240.

(19) Wyles, L. R.; Nordeen, D. H.; Hitchcock, R. H.; Gladon, R. J.; Hawbecker, B. L. *Ohio J. Sci.* **1972**, *72*, 276−284.

(20) (a) Sheldrick, G. M. *Acta Crystallogr., Sect. A* **2008**, *64*, 112. (b) Sheldrick, G. M. *SHELXL-2013*; University of Göttingen, Göttingen, Germany, 2013.

(21) Dolomanov, O. V.; Bourhis, L. J.; Gildea, R. J.; Howard, J. A. K.; Puschmann, H. J. *Appl. Crystallogr.* **2009**, *42*, 339−341.

DOI: 10.1021/acs.organomet.5b00295
Organometallics XXXX, XXX, XXX−XXX